

- Electronic Supplementary Information -

Substituent-Controlled Racemization of Coordination Capsules

Kentaro Harada, Ryo Sekiya, Takeshi Maehara, and Takeharu Haino *

¹ Department of Chemistry, Graduate School of Science, Hiroshima University, 1-3-1 Kagamiyama,
Higashi-Hiroshima, Hiroshima 739-8526, Japan

To whom correspondence should be addressed

haino@hiroshima-u.ac.jp

Contents

Compound Characterizations

• Figure S1	¹ H and ¹³ C NMR spectra of 7 in chloroform- <i>d</i> ₁	… S3
• Figure S2	¹ H and ¹³ C NMR spectra of 2c in chloroform- <i>d</i> ₁	… S3
• Figure S3	¹ H and ¹³ C NMR spectra of 9 in chloroform- <i>d</i> ₁	… S4
• Figure S4	DQF-COSY spectrum of 2c in chloroform- <i>d</i> ₁	… S4
• Figure S5	NOESY spectrum of 2c in chloroform- <i>d</i> ₁	… S5

Supporting Figures and Tables

• Figure S6.	Change of the ¹ H NMR spectra of 2c before and after addition of Cu ⁺	… S6
• Figure S7.	Change of the ¹ H NMR spectra of 9 before and after addition of Cu ⁺	… S6
• Figure S8.	DQF-COSY spectrum of 1c in chloroform- <i>d</i> ₁	… S7
• Figure S9.	NOESY spectrum of 1c in chloroform- <i>d</i> ₁	… S7
• Figure S10.	¹ H NMR spectra of the mixtures of 1b and <i>rac</i> - 3 in chloroform- <i>d</i> ₁	… S8
• Figure S11.	¹ H NMR spectra of the mixtures of 1c and <i>rac</i> - 3 in chloroform- <i>d</i> ₁	… S8
• Figure S12.	¹ H NMR spectra of the mixtures of 1d and <i>rac</i> - 3 in chloroform- <i>d</i> ₁	… S8
• Figure S13.	Line fitting of the signals of the bound guests in 1b–1d	… S9
• Figure S14.	¹ H NMR spectra of the mixtures of 1b and (<i>R</i>)- 3 in chloroform- <i>d</i> ₁	… S9
• Figure S15.	¹ H NMR spectra of the mixtures of 1c and (<i>R</i>)- 3 in chloroform- <i>d</i> ₁	… S9
• Figure S16.	¹ H NMR spectra of the mixtures of 1d and (<i>R</i>)- 3 in chloroform- <i>d</i> ₁	… S10
• Figure S17.	UV-vis absorption spectra of 1a–d and 4a–d in THF	… S10
• Figure S18.	¹ H NMR spectra of the mixtures of the enantiomerically enriched coordination capsule and (<i>R</i>)- 3 in chloroform- <i>d</i> ₁	… S11
• Figure S19.	ORTEP drawings of 4c and optimized structure of 4c	… S11
• Figure S20.	Calculation of the racemization constant (<i>k</i> _{rac}) of 1d in THF	… S12
• Table S1.	Bond lengths and angles of the Cu(I) centers of 4c in the solid state and the optimized structure of 4c	… S12
• Table S2.	Cartesian coordinate of the optimized structure of 4c	… S13–S14
• Figure S21.	¹ H and ¹³ C NMR spectra of 1c in chloroform- <i>d</i> ₁	… S15
• Figure S22.	¹ H and ¹³ C NMR spectra of 4c in chloroform- <i>d</i> ₁	… S15

References

• References	… S16
---------------------	-------

Compound Characterization Section

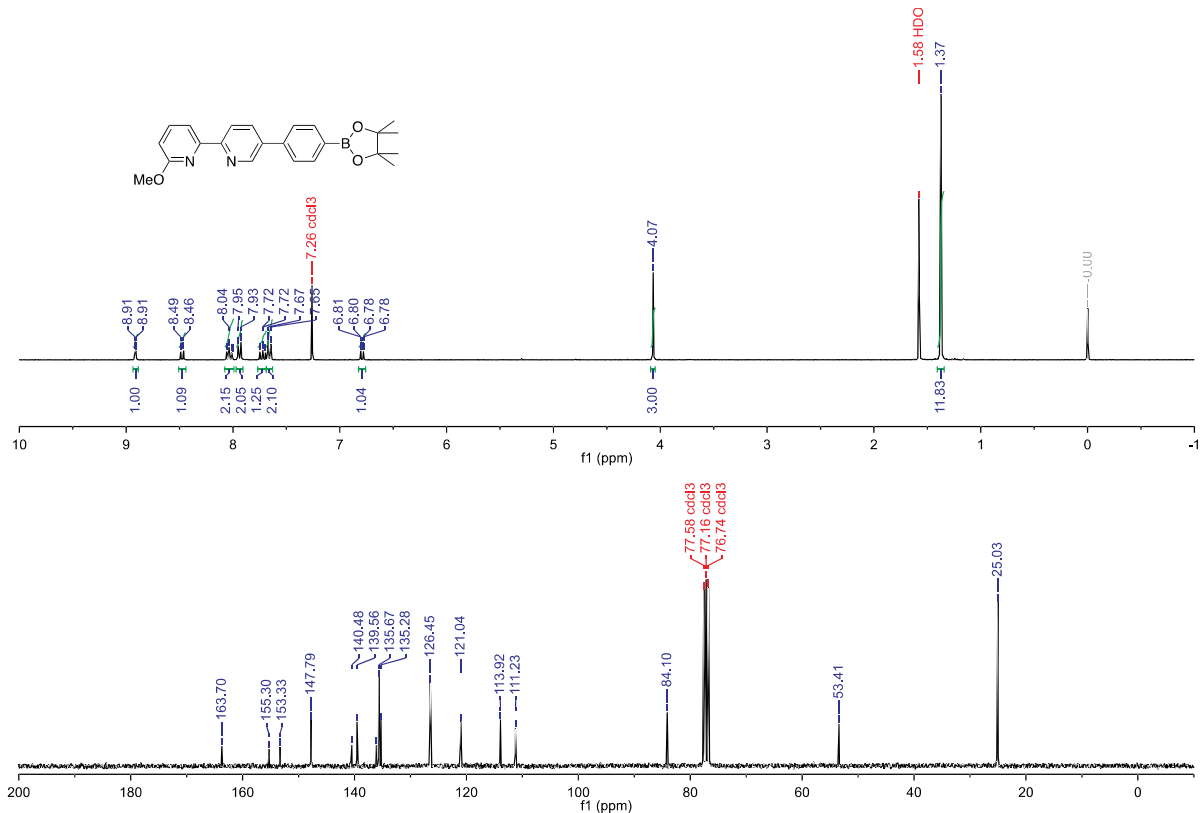


Figure S1. ^1H (300 MHz, chloroform- d_1 , 293 K) and ^{13}C (75 MHz, chloroform- d_1 , 293 K) NMR spectra of **7**.

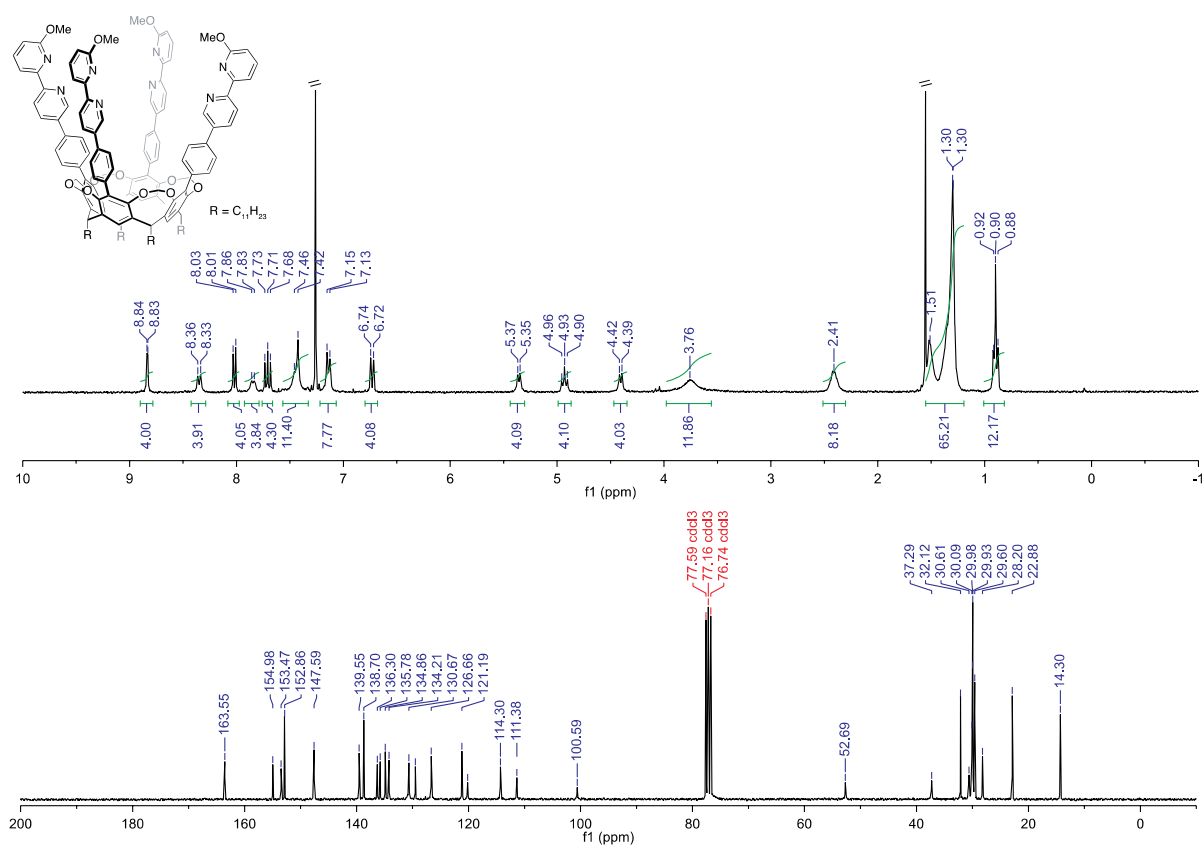


Figure S2. ^1H (300 MHz, chloroform- d_1 , 293 K) and ^{13}C (75 MHz, chloroform- d_1 , 293 K) NMR spectra of **2c**.

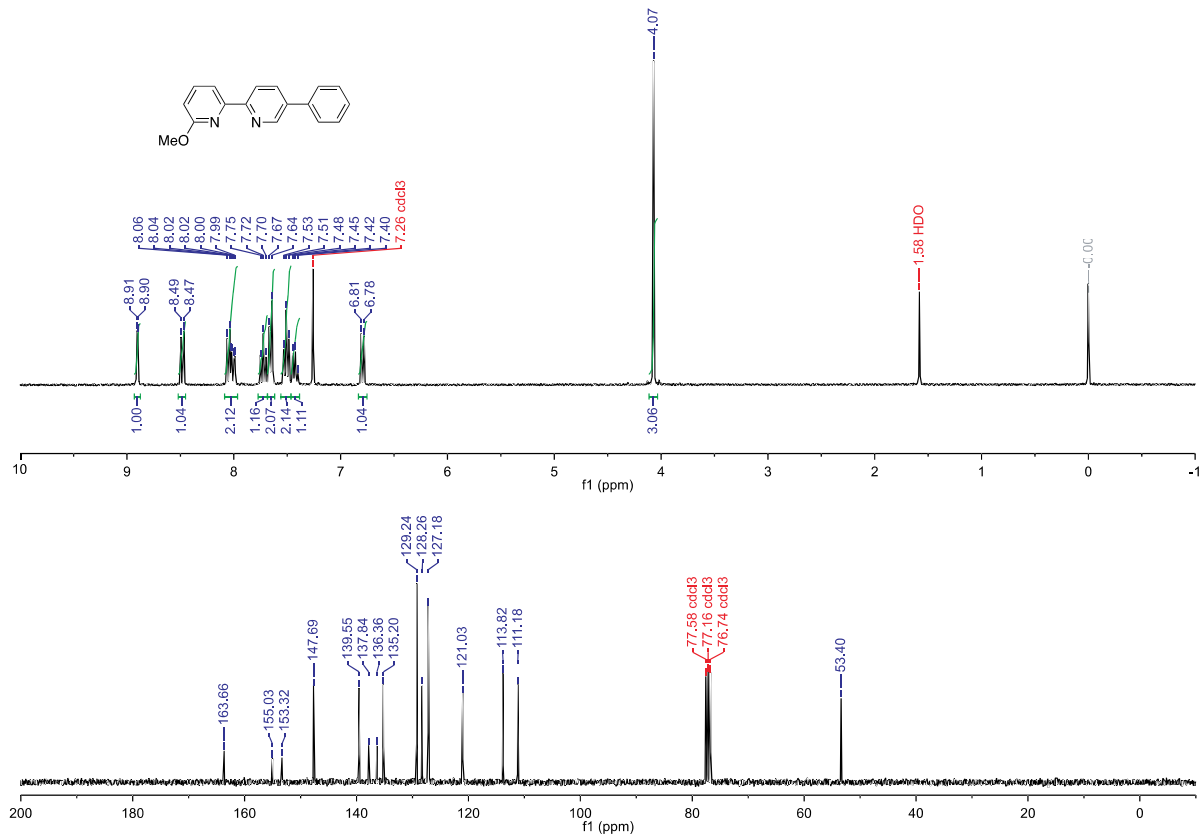


Figure S3. ^1H (300 MHz, chloroform- d_1 , 293 K) and ^{13}C (75 MHz, chloroform- d_1 , 293 K) NMR spectra of **9**.

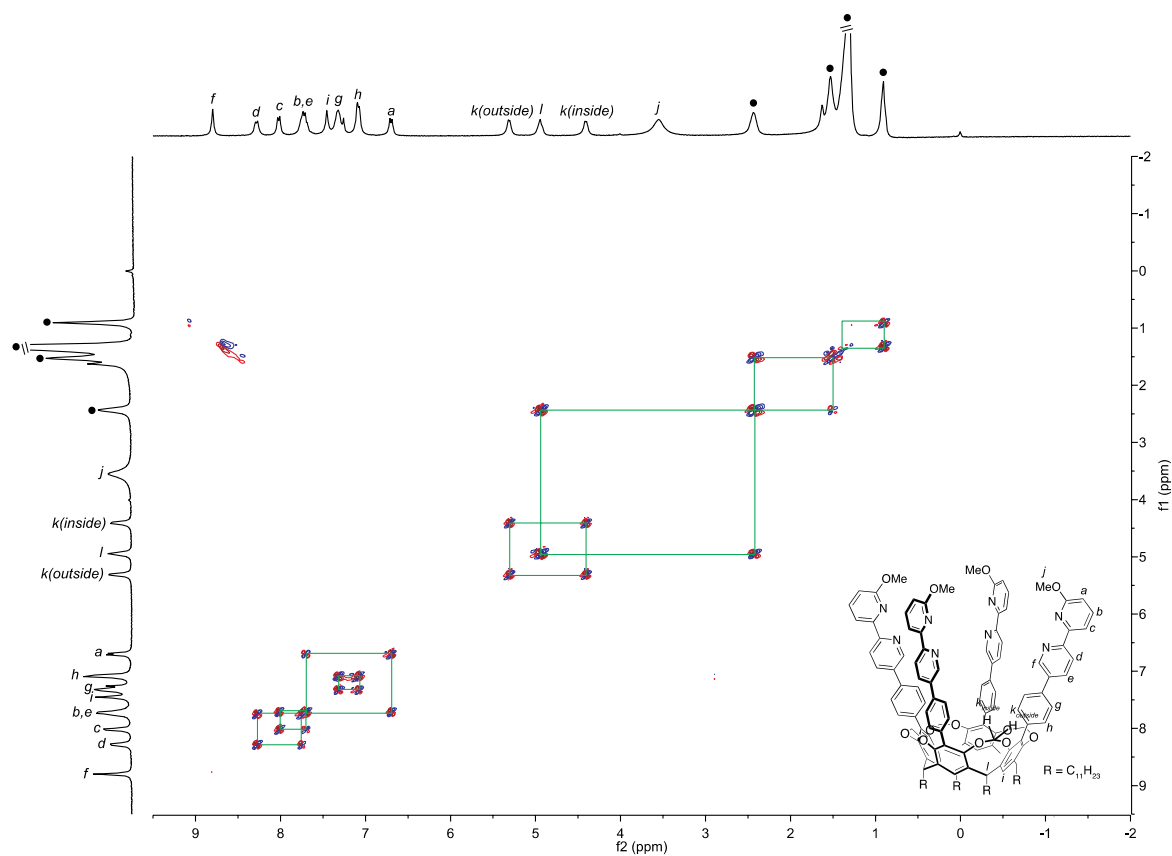


Figure S4. DQF-COSY spectrum (300 MHz, chloroform- d_1 , 293 K) of **2c**.

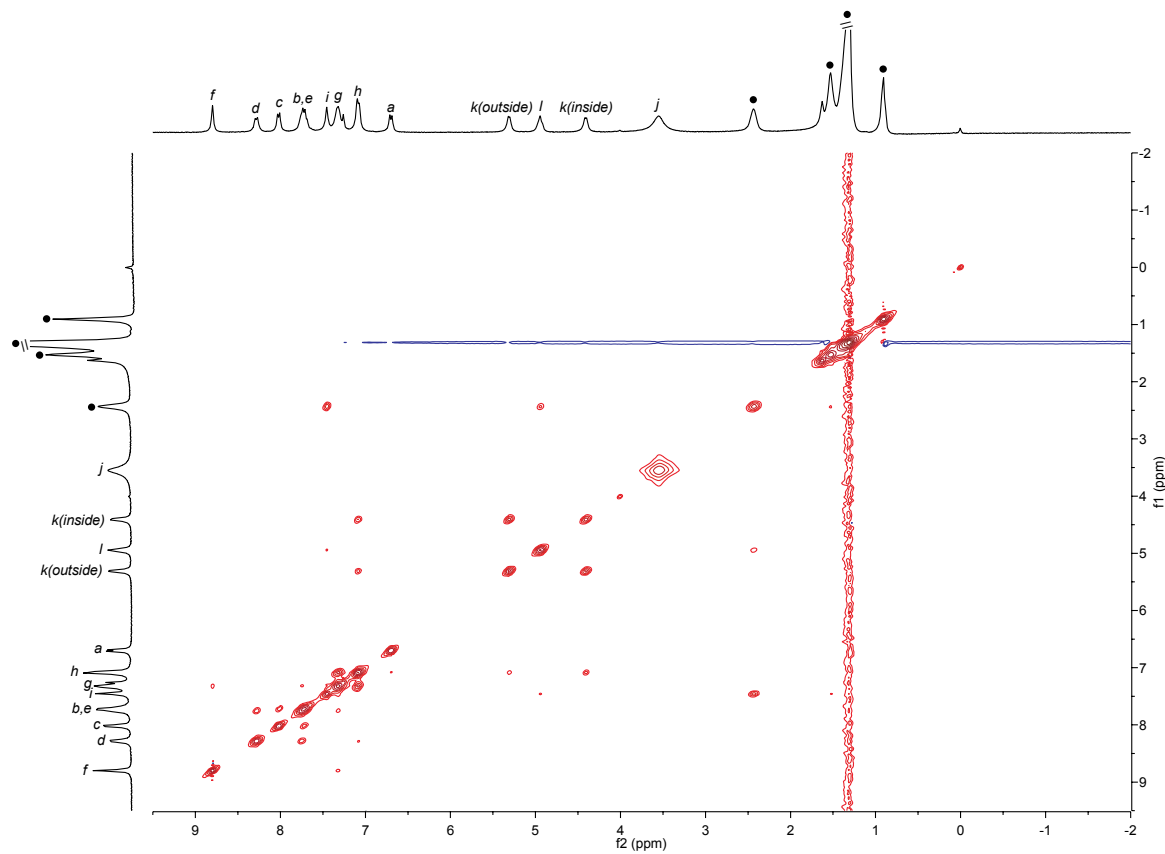


Figure S5. NOESY spectrum (300 MHz, chloroform- d_1 , 293 K) of **2c**. Mixing time = 400 ms.

Supporting Figures and Tables

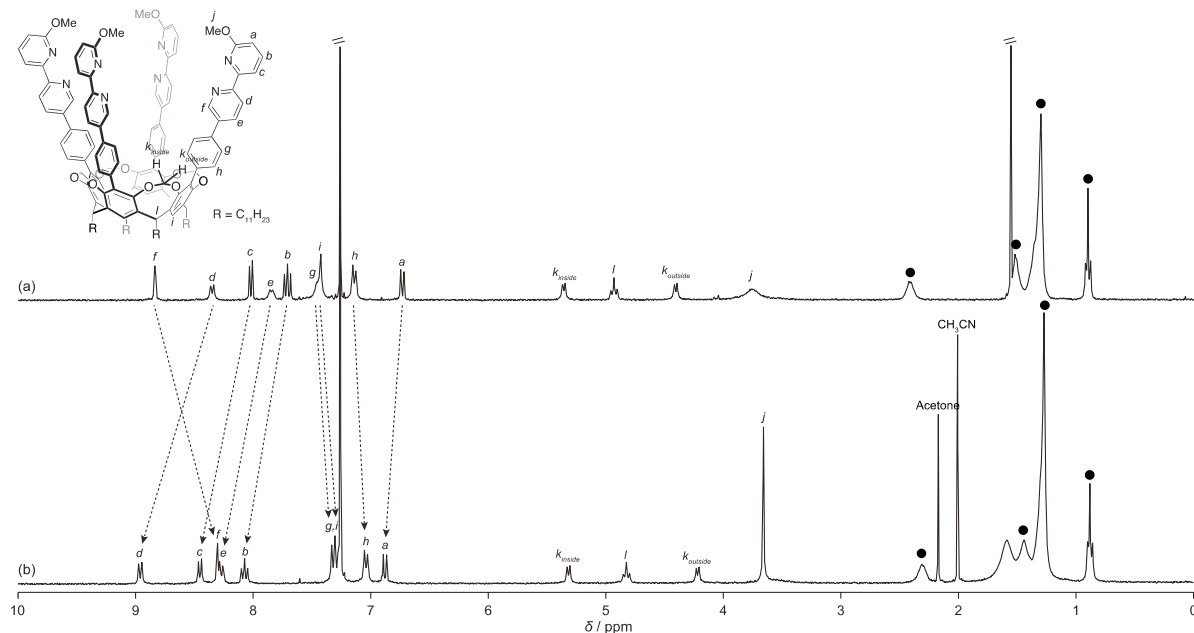


Figure S6. ^1H NMR spectra (300 MHz, chloroform- d_1 , 293 K) of **2c** (a) before and (b) after addition of 2 equiv. of $[\text{Cu}(\text{NCCH}_3)_4]\text{BF}_4$.

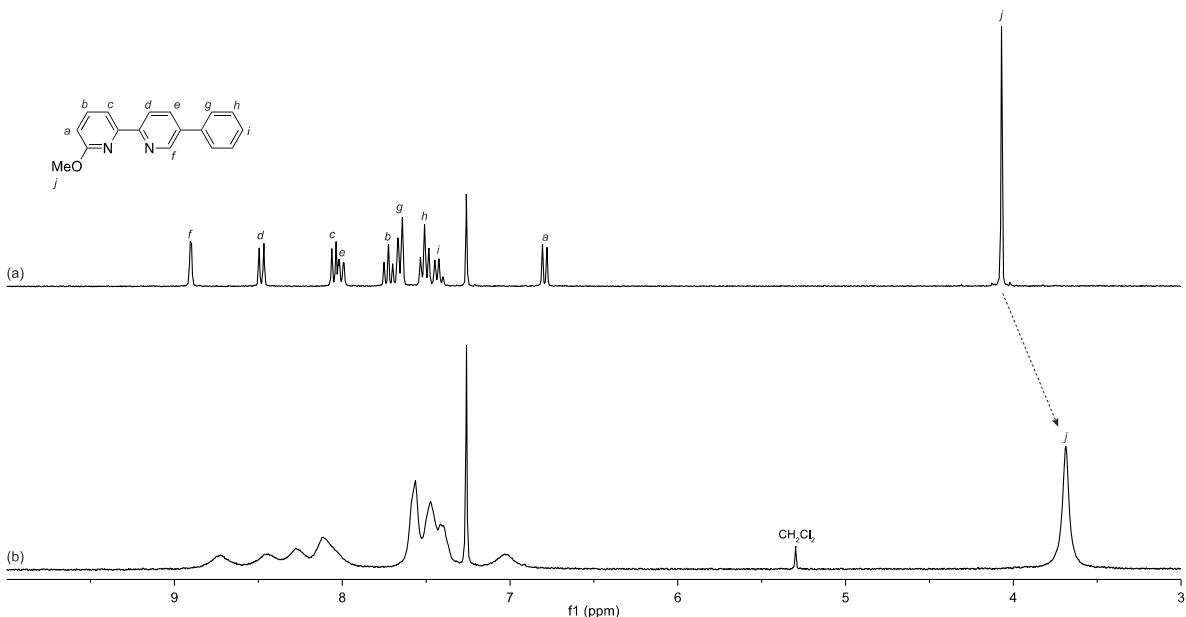


Figure 7. ^1H NMR spectra (300 MHz, chloroform- d_1 , 293 K) of **9** (a) before and (b) after addition of 0.5 equiv. of $[\text{Cu}(\text{NCCH}_3)_4]\text{BF}_4$.

The signals changes of **2c** are commonly observed in the formation of the coordination capsules (Figure S6).^[1] The number of the signals remained unchanged. That indicates the D_4 symmetry of capsule **1c** on the NMR time scale. The signals of **9** broadened after the complexation (Figure S7). The upfield shift of Hj indicates that the methoxy group exists near the aromatic ring. This picture is consistent with the X-ray crystal structure of **1c** wherein the methoxy group lies on the bipyridine moiety.

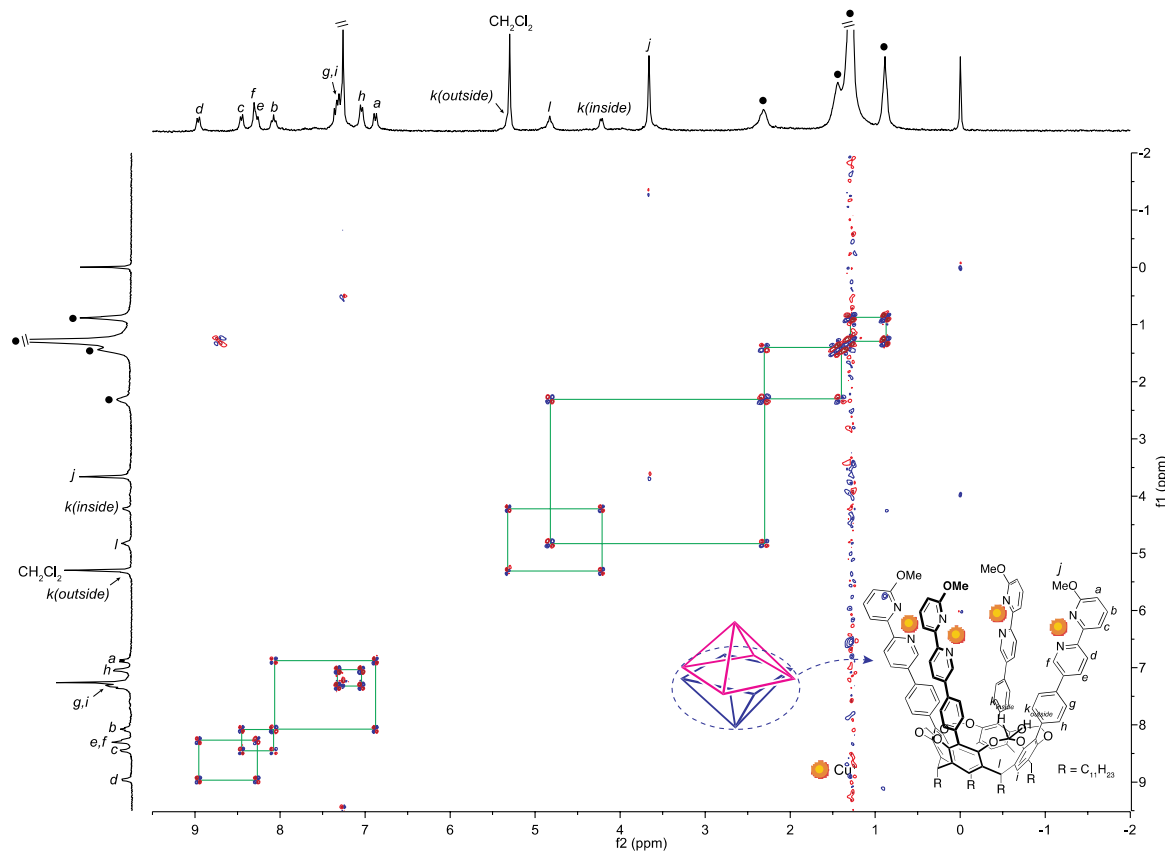


Figure S8. DQF-COSY spectrum (300 MHz, chloroform- d_1 , 293 K) of **1c**.

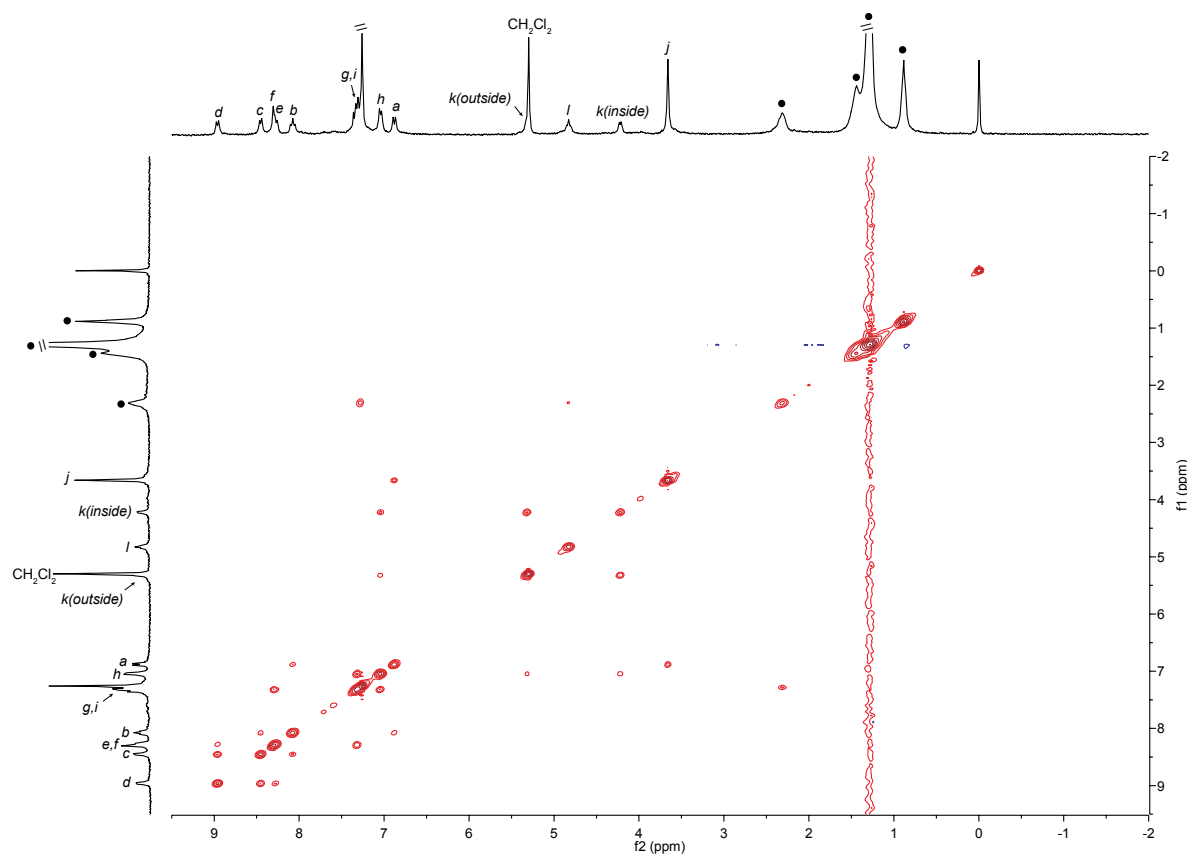


Figure S9. NOESY spectrum (300 MHz, chloroform- d_1 , 293 K) of **1c**. Mixing time = 400 ms.

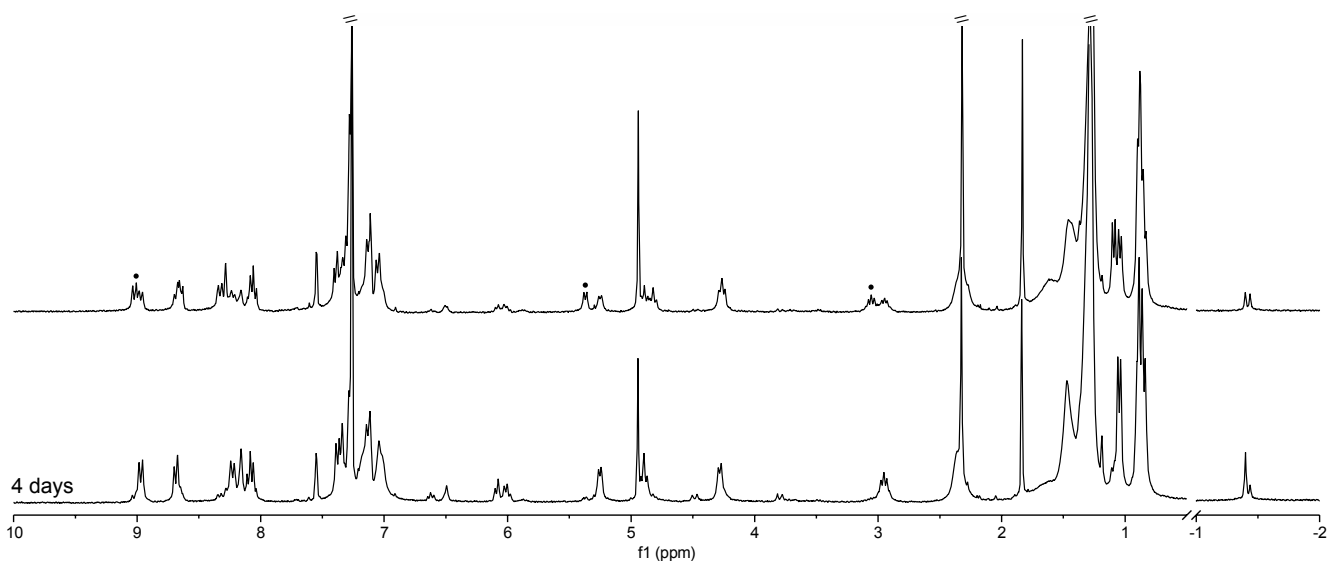


Figure S10. ¹H NMR spectra (300 MHz, chloroform-*d*₁, 293 K) of a mixture of **1b** + *rac*-**3**. Filled circles denote free **1b**.

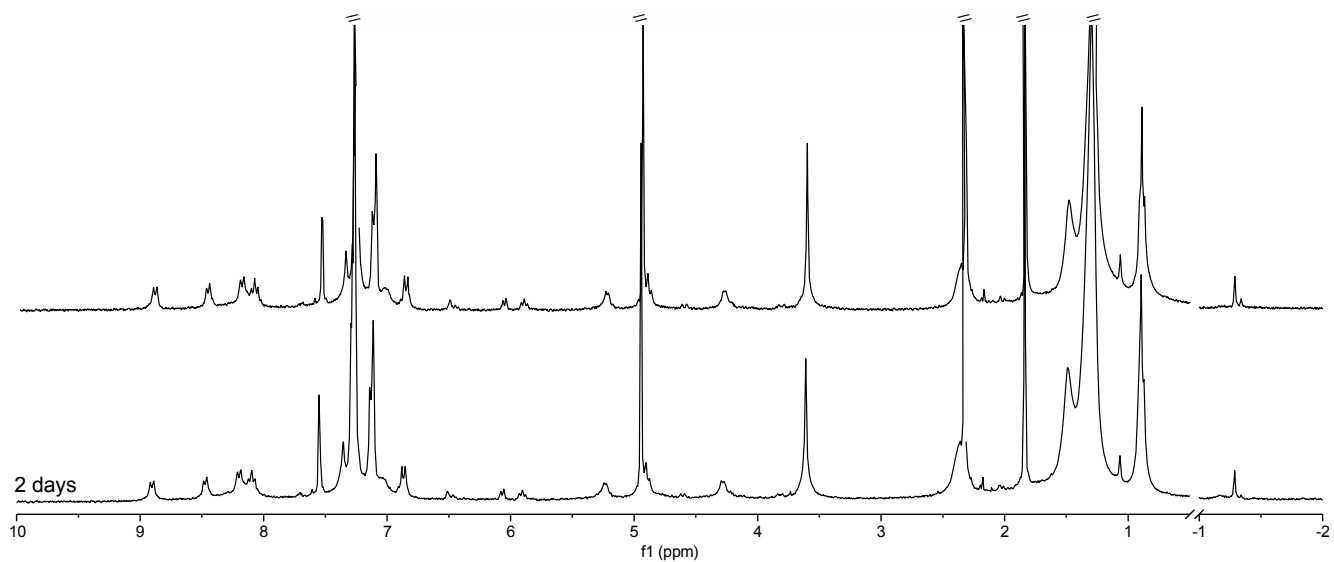


Figure S11. ¹H NMR spectra (300 MHz, chloroform-*d*₁, 293 K) of a mixture of **1c** + *rac*-**3**.

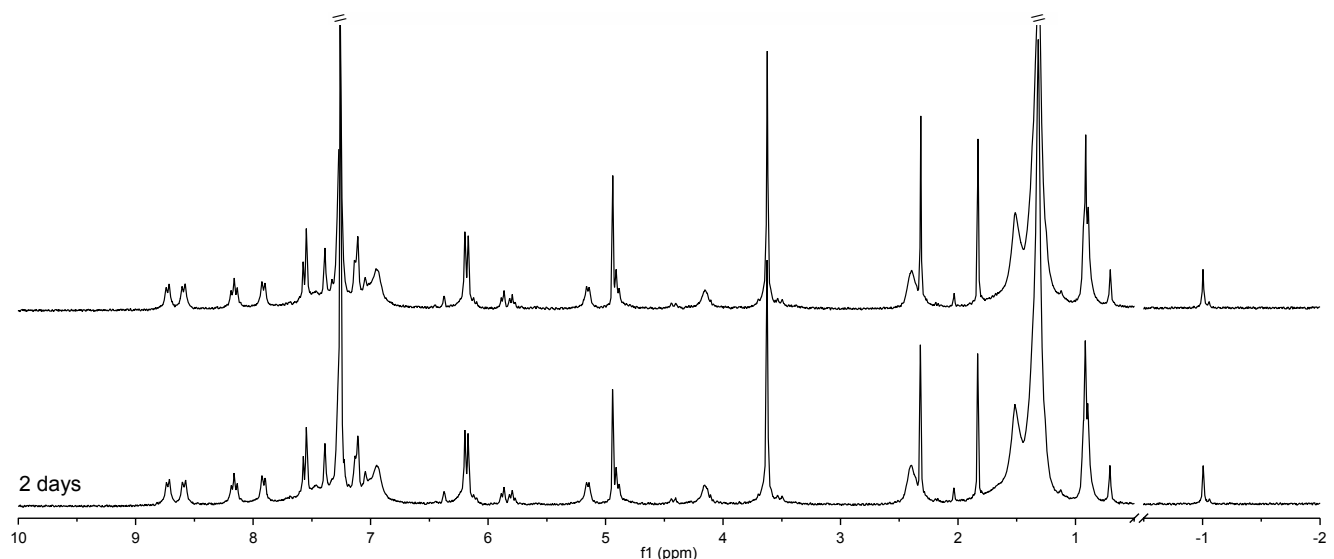


Figure S12. ¹H NMR spectra (300 MHz, chloroform-*d*₁, 293 K) of a mixture of **1d** + *rac*-**3**.

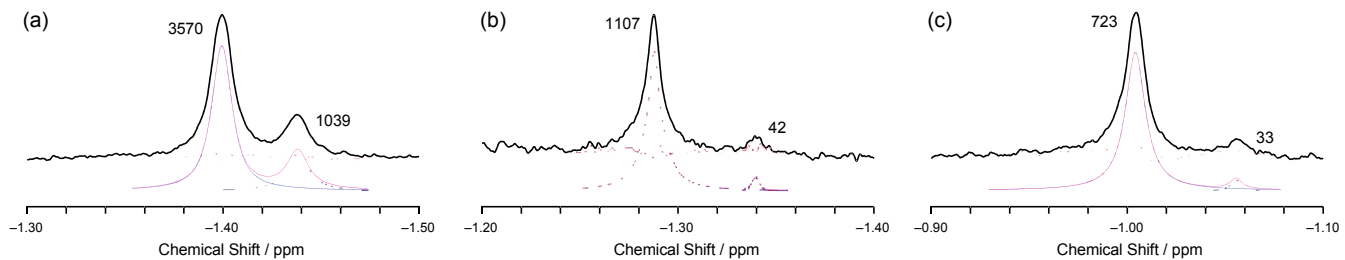


Figure S13. Line fitting of the signals of the bound guest in predominant and subordinate host-guest complexes. (a) **1b** and *rac*-**3**, (b) **1c** and *rac*-**3**, and (c) **1d** and *rac*-**3**. In (a)–(c), figures indicate the relative area of the predominant and subordinate species. The diastereomeric excess was calculated to be 55 de% (**1b**), 93 de% (**1c**), and (c) 91% (**1d**). based on the relative signal intensities of the predominant and subordinate diastereomers.

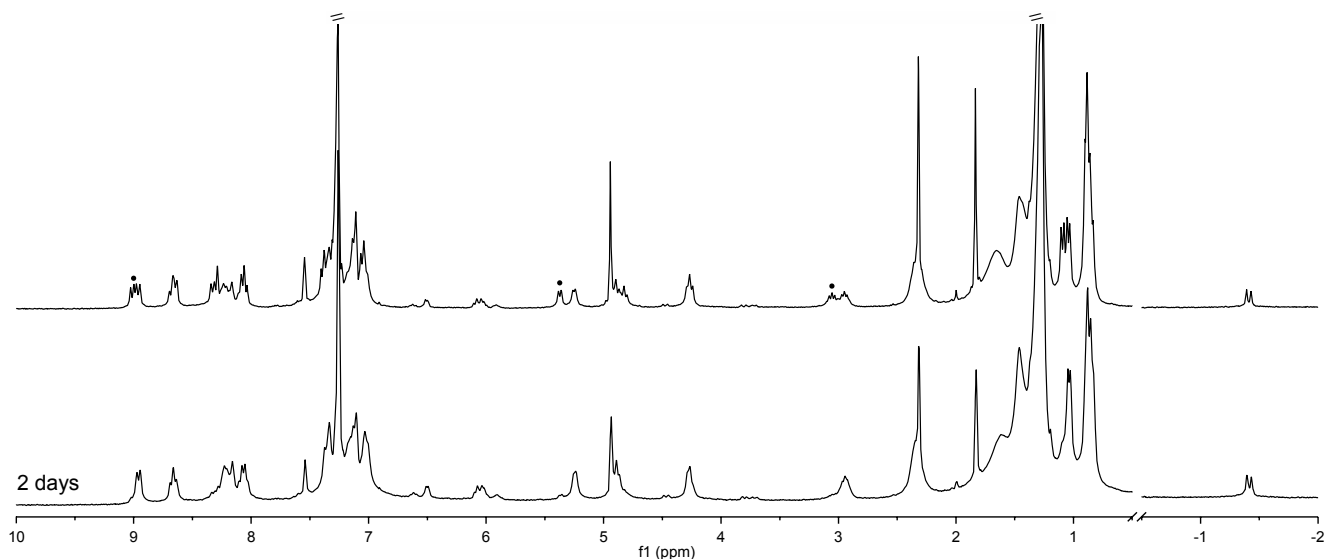


Figure S14. ^1H NMR spectra (300 MHz, chloroform- d_1 , 293 K) of a mixture of **1b** and (*R*)-**3**. Filled circles denote free **1b**.

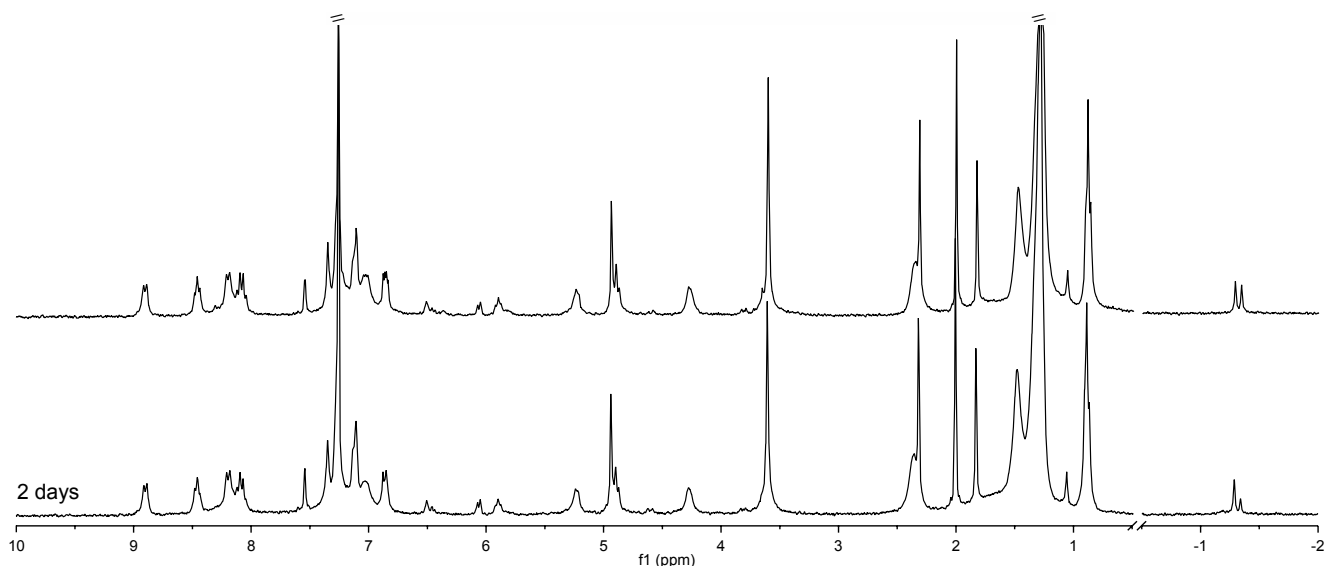


Figure S15. ^1H NMR spectra (300 MHz, chloroform- d_1 , 293 K) of a mixture of **1c** and (*R*)-**3**.

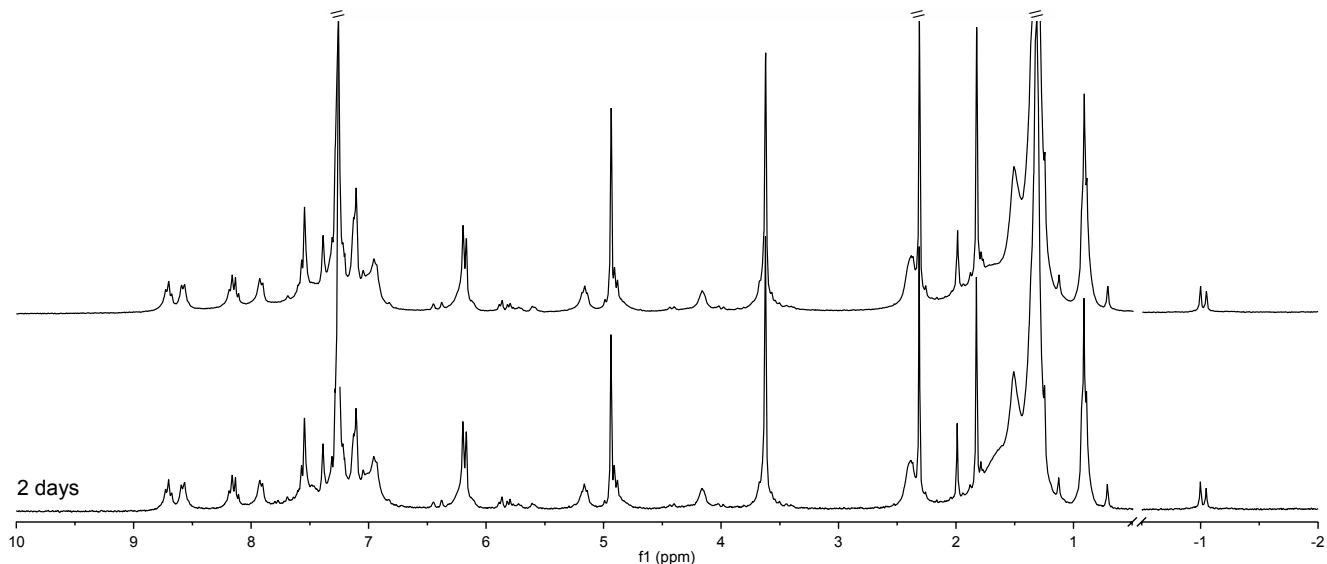


Figure S16. ^1H NMR spectra (300 MHz, chloroform- d_1 , 293 K) of a mixture of **1d** and (*R*)-**3**.

Figures S10 and S14 show that the free capsule still exists in the solution, while none of signals corresponding to the free capsules was detected in Figures S11, S12, S15, and S17. These observations indicate that **1c** and **1d** formed the host-guest complexes with the given guests immediately after mixing the capsule and the guest, while **1b** did not.

Figures S11 and S12 show the formation of the specific diastereomeric pair just after mixing the capsule and the guest, while Figures S15 and S16 demonstrate that the ratio of the diastereomers was gradually changed (**1b**: 5 de% \rightarrow 21 de%; **1c**: 5 de% \rightarrow 42 de%). These results indicate the rapid exchange between bound and unbound guests, while the slow helicity inversion of the coordination capsules in chloroform- d_1 .

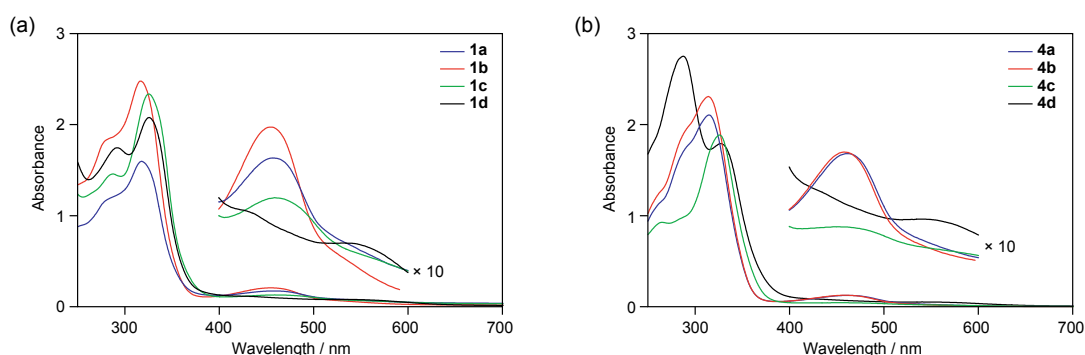


Figure S17. UV-vis absorption spectra (THF, 293 K) of (a) **1a–d** and (b) **4a–d** in chloroform. The concentrations of **1a–d** are $1.0 \times 10^{-5} \text{ M}^{-1}$ and those of **4a–d** are $5.0 \times 10^{-5} \text{ M}^{-1}$. The λ_{max} of the MLCT bands are 458 (**1a**), 453 (**1b**), 467 (**1c**), 545 (**1d**), 462 (**4a**), 458 (**4b**), 469 (**4c**), and 547 nm (**4d**).

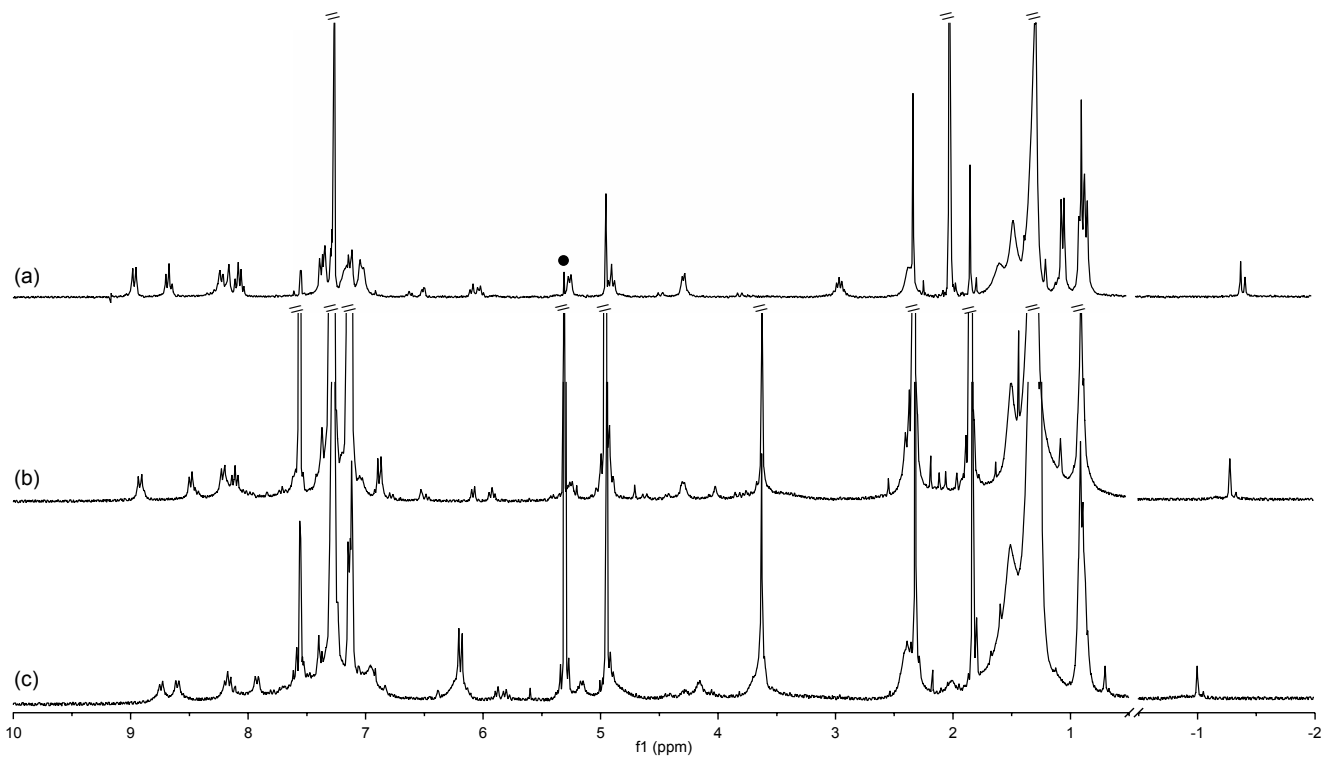


Figure S18. (a)-(c) ¹H NMR spectra (300 MHz, chloroform-*d*₁, 293 K) of the mixtures of the enantiomerically enriched coordination capsules (**1b-d**) and (*R*)-**3**. (a) **1b** and (*R*)-**3**, (b) **1c** and (*R*)-**3**, and (c) (a) **1d** and (*R*)-**3**. The diastereomeric excess was calculated to be 32 de% (**1b**), 81 de% (**1c**), and 75 de% (**1d**) based on the relative signal intensities of the predominant and subordinate diastereomers. Filled circles denote dichloromethane.

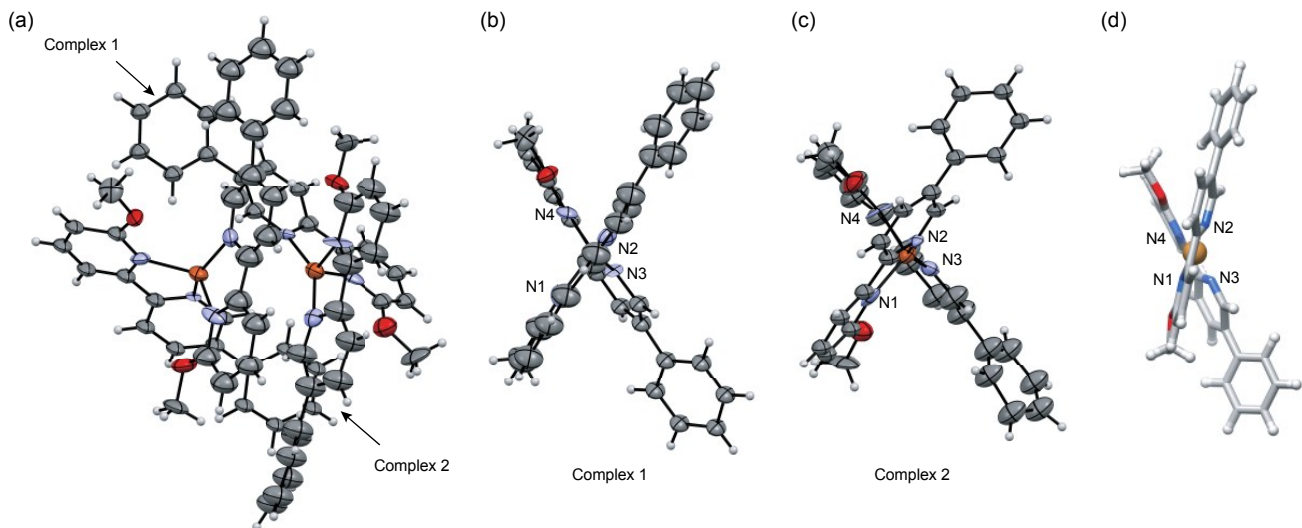


Figure S19. (a)-(c) ORTEP drawing of the X-ray crystal structures of **4c**. (a) Dimer, (b) complex A, and (c) complex B. (d) An optimized structure of **4c** at the M06-2X/6-31G(d,p)+LanL2DZ level of theory. Color scheme in (a)-(d): gray (carbon), white (hydrogen), light blue (nitrogen), red (oxygen), orange (copper).

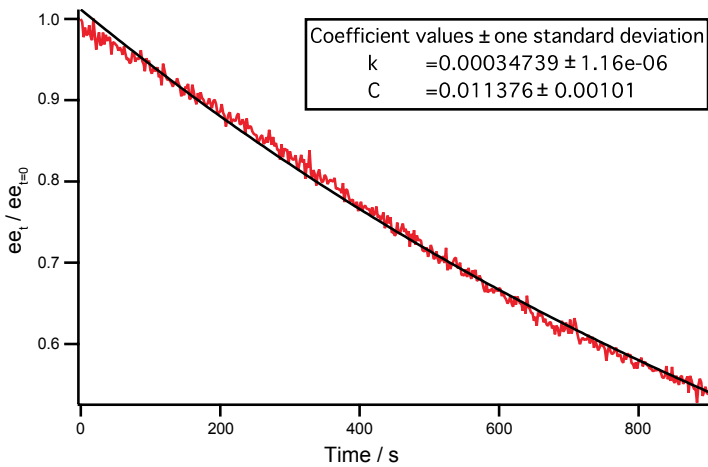


Figure S20. Calculation of the rate of the racemization (krac) of **1d** in THF. Red (observed), black (calculation).

Table S1. Bond lengths (Å) and angles (°) of the Cu(I) center of **4c** in the solid state and the optimized structure of **4c**.

	4c (complex 1) ^[a]	4c (complex 2) ^[a]	4c (optimized structure) ^[a]
Cu–N1 / Å	2.080(15)	2.051(15)	2.140
Cu–N2 / Å	1.995(13)	2.007(12)	2.179
Cu–N3 / Å	1.987(12)	1.985(14)	2.153
Cu–N4 / Å	2.046(13)	2.061(14)	2.161
N1–Cu–N2 / °	81.1(6)	80.6(6)	146.36
N1–Cu–N3 / °	114.7(5)	115.6(6)	118.38
N2–Cu–N3 / °	145.3(5)	149.3(5)	76.79
N2–Cu–N4 / °	119.0(5)	114.9(5)	108.8
N3–Cu–N4 / °	79.8(5)	82.0(6)	144.48
N4–Cu–N1 / °	122.9(6)	117.2(6)	76.95

[a] The atomic numbering scheme is shown in Figure S19.

Table S2. Cartesian coordinates of the optimized structure of **4c** at M06-2X/6-31G(d,p)+LanL2DZ level of theory.^[2]

Center Number	Atomic Number	Atomic Type	Coordinates (Angstroms)		
			X	Y	Z
1	6	0	7.752304	0.144788	-2.166838
2	1	0	8.672544	0.540520	-2.582963
3	6	0	7.505638	-1.225573	-2.195087
4	1	0	8.229077	-1.900042	-2.640632
5	6	0	6.327011	-1.734279	-1.661390
6	1	0	6.128225	-2.800794	-1.713206
7	6	0	5.378881	-0.877714	-1.091090
8	6	0	5.635158	0.498117	-1.068986
9	1	0	4.912489	1.170105	-0.613801
10	6	0	6.813557	1.005807	-1.603444
11	1	0	7.003868	2.073563	-1.575074
12	6	0	4.124591	-1.414306	-0.520984
13	6	0	4.065705	-2.644826	0.138619
14	1	0	4.969480	-3.232000	0.270758
15	6	0	2.860335	-3.098766	0.655311
16	1	0	2.817590	-4.038315	1.193501
17	6	0	1.721768	-2.306563	0.515656
18	6	0	0.391079	-2.711579	1.048323
19	6	0	0.071059	-4.032746	1.347368
20	1	0	0.786555	-4.830612	1.195955
21	6	0	-1.213171	-4.307785	1.809359
22	1	0	-1.497762	-5.327465	2.046957
23	6	0	-2.138454	-3.285326	1.957916
24	1	0	-3.139604	-3.486976	2.314804
25	6	0	-1.725089	-1.987572	1.630175
26	6	0	2.927772	-0.694532	-0.611673
27	1	0	2.899358	0.261597	-1.126886
28	6	0	-3.890108	-1.074298	1.958368
29	1	0	-4.338849	-1.723564	1.197667
30	1	0	-4.331238	-0.080510	1.887499
31	1	0	-4.070100	-1.484405	2.957125
32	6	0	-7.434718	-1.357296	-2.074101
33	1	0	-8.291850	-1.961130	-2.352287

34	6	0	-7.543590	-0.423638	-1.046130
35	1	0	-8.483495	-0.303226	-0.517847
36	6	0	-6.446616	0.354030	-0.691659
37	1	0	-6.531219	1.067565	0.123752
38	6	0	-5.226517	0.207209	-1.362148
39	6	0	-5.126468	-0.733540	-2.393653
40	1	0	-4.194325	-0.833805	-2.942323
41	6	0	-6.224950	-1.509809	-2.747076
42	1	0	-6.138878	-2.226990	-3.556455
43	6	0	-4.056383	1.021575	-0.968228
44	6	0	-2.776338	0.459162	-0.922404
45	1	0	-2.629093	-0.587192	-1.180725
46	6	0	-4.165999	2.360153	-0.581414
47	1	0	-5.132792	2.854029	-0.607800
48	6	0	-3.037937	3.057655	-0.172647
49	1	0	-3.123398	4.087578	0.152889
50	6	0	-1.805797	2.403993	-0.156125
51	6	0	-0.556200	3.063194	0.317990
52	6	0	-0.418244	4.445367	0.406772
53	1	0	-1.212869	5.110040	0.093490
54	6	0	0.784559	4.954895	0.887696
55	1	0	0.924438	6.027436	0.973389
56	6	0	1.814052	4.098989	1.250546
57	1	0	2.751723	4.485414	1.626506
58	6	0	1.592679	2.724237	1.101069
59	6	0	3.742449	2.166473	1.935413
60	1	0	4.287417	2.837184	1.262124
61	1	0	4.311386	1.247366	2.069879
62	1	0	3.595687	2.654831	2.904012
63	7	0	1.772399	-1.118282	-0.106500
64	7	0	-0.498908	-1.719141	1.192428
65	7	0	-1.691946	1.121138	-0.530169
66	7	0	0.438886	2.232577	0.661108
67	8	0	-2.501743	-0.896490	1.717840
68	8	0	2.499979	1.771005	1.372212
69	29	0	0.081539	0.155747	0.287869

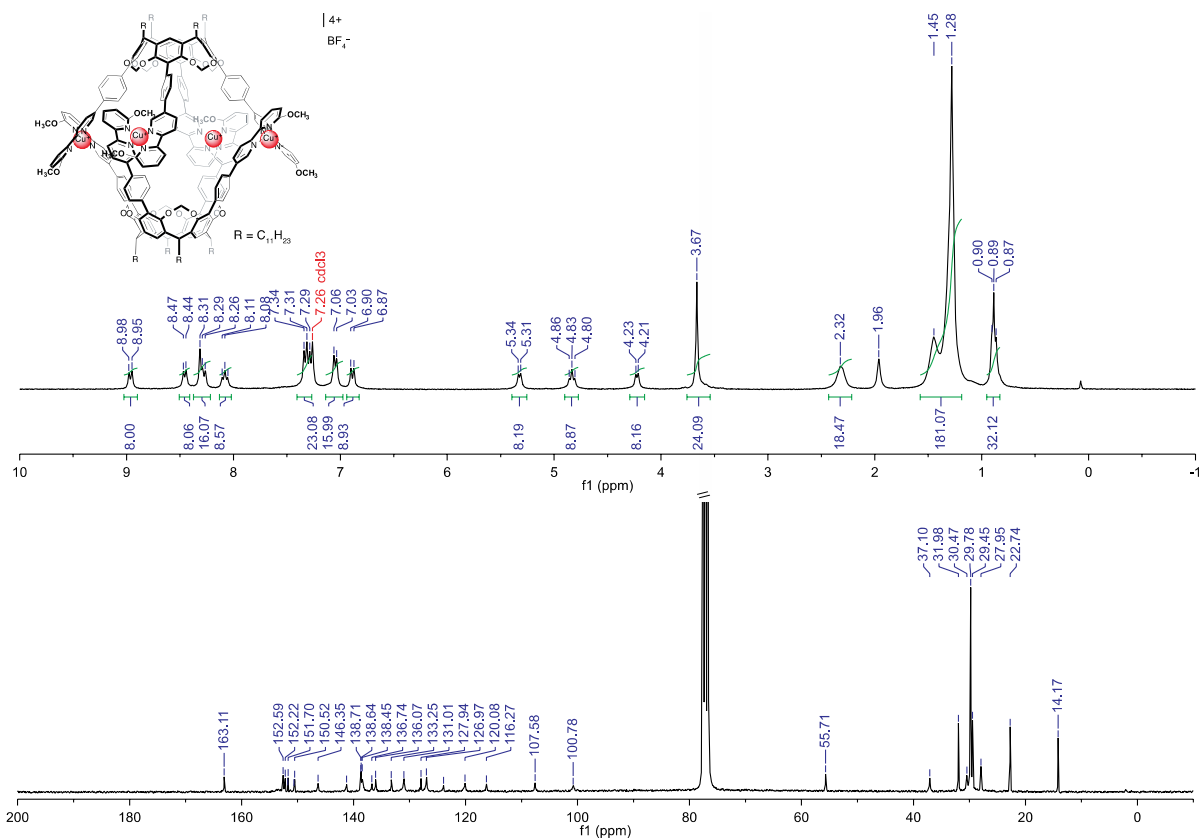


Figure S21. ^1H (300 MHz, chloroform- d_1 , 293 K) and ^{13}C (75 MHz, chloroform- d_1 , 293 K) NMR spectra of **1c**.

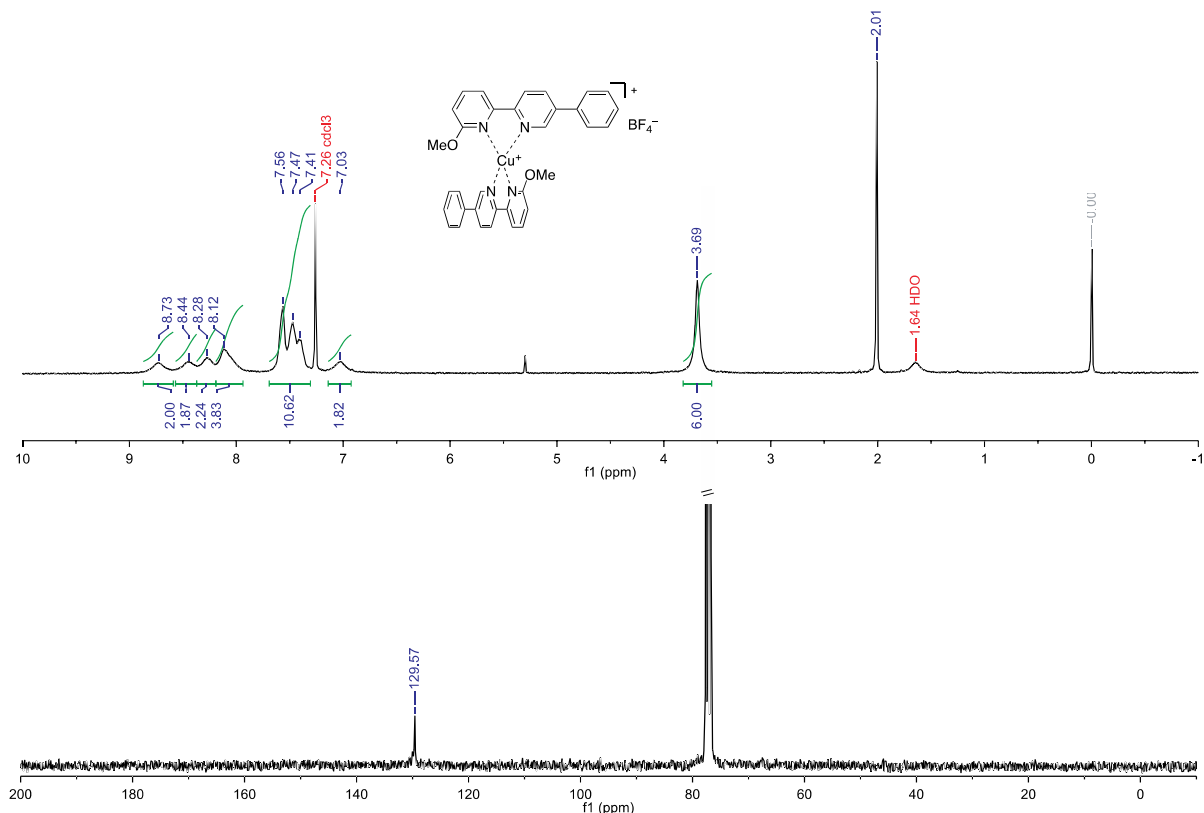


Figure S22. ^1H (300 MHz, chloroform- d_1 , 293 K) and ^{13}C (75 MHz, chloroform- d_1 , 293 K) NMR spectra of **4c**.

References

- [1] T. Imamura, T. Machara, R. Sekiya, and T. Haino, *Chem. Eur. J.*, **2016**, 22, 3250–3254.
- [2] *Gaussian 09*, Revision D.01, M. J. Frisch, G. W. Trucks, H. B. Schlegel, G. E. Scuseria, M. A. Robb, J. R. Cheeseman, G. Scalmani, V. Barone, B. Mennucci, G. A. Petersson, H. Nakatsuji, M. Caricato, X. Li, H. P. Hratchian, A. F. Izmaylov, J. Bloino, G. Zheng, J. L. Sonnenberg, M. Hada, M. Ehara, K. Toyota, R. Fukuda, J. Hasegawa, M. Ishida, T. Nakajima, Y. Honda, O. Kitao, H. Nakai, T. Vreven, J. A. Montgomery, Jr., J. E. Peralta, F. Ogliaro, M. Bearpark, J. J. Heyd, E. Brothers, K. N. Kudin, V. N. Staroverov, R. Kobayashi, J. Normand, K. Raghavachari, A. Rendell, J. C. Burant, S. S. Iyengar, J. Tomasi, M. Cossi, N. Rega, J. M. Millam, M. Klene, J. E. Knox, J. B. Cross, V. Bakken, C. Adamo, J. Jaramillo, R. Gomperts, R. E. Stratmann, O. Yazyev, A. J. Austin, R. Cammi, C. Pomelli, J. W. Ochterski, R. L. Martin, K. Morokuma, V. G. Zakrzewski, G. A. Voth, P. Salvador, J. J. Dannenberg, S. Dapprich, A. D. Daniels, Ö. Farkas, J. B. Foresman, J. V. Ortiz, J. Cioslowski, and D. J. Fox, Gaussian, Inc., Wallingford CT, **2009**.